

Profound Shift of Thrust Line of Masonry Vault Through Boundary Condition and Modelling Strategy for Structural Stability Study Using FETLA: Real Life Example

Varma Varad
Civil Department
JNEC, MG MU
Chh. Sambhajinagar, India

J. P. Bhandari
Civil Department
JNEC, MG MU
Chh. Sambhajinagar, India

Abstract - Because the vault structure has a lot of redundancy, there are many possible equilibrium solutions. Conventional Finite Element Analysis (FEA) provides a singular solution focused on minimizing strain energy, neglecting the varying modulus of elasticity under tension and compression, as typically exhibited by masonry structures. When studying masonry vaults, it's important to keep in mind the main properties of the material "masonry," such as its heterogeneity, low resistance to tension, good compressive strength, and high friction coefficient. It's also important to remember how important the overall shape is for achieving equilibrium. This study presents a structural assessment of a 9-meter Spanning Un-Reinforced Masonry (URM) vault at a library building under construction using stone and lime at Wani, Nashik, India. The primary objective is to evaluate the vault's structural response to self-weight and superimposed loads under varying boundary conditions. The results show that changes in boundary conditions and modeling approach modify the Thrust Line, which affects load-bearing efficiency and how structural integrity is interpreted. This large variations in FEA results necessitate the need for modification in conventional FEA to incorporate different material behavior in tension and compression, and also gives necessary insight on effect of modelling strategy on stability study

Keywords - *Vault, Finite Element, Manonry, Thrust Line, FETLA*

Although unreinforced masonry structures are common in both historical and modern architecture, their brittle nature, anisotropic material properties, and nonlinear response to loading make them intrinsically complex. The distribution of internal forces and the thrust line's location, which determines stability, have a significant impact on how these structures behave.

It is well known that rather than compressive material failure, URM vaults fail mainly because of geometric instability (different from classical buckling) resulting from their incapacity to withstand tensile stresses (Heyman, 1966; Clemente et al., 1995; Block et al., 2006; Zessim et al., 2010). The stability of such vaults depends critically on the Thrust Line, a theoretical representation of compressive force flow remaining within the masonry section. Progressive collapse may result from localized cracking and hinge formations when the thrust line deviates beyond the middle third of the vault's thickness.

This paper presents the structural analysis of a (URM) segmental vault constructed with Jodhpur sandstone of a Library Building in Wani (Maharashtra, India). Because of its segmental geometry, the vault's low-rise, singly curved profile is optimized for compressive load transfer. With a clear span of 9 meters, a maximum rise of 0.9 meters, and a constant thickness 0.6 meters at the base and at the crown.

The purpose of this study is to use Finite Element Analysis (FEA) and Finite Element Thrust Line Analysis (FETLA) to examine how the vault responds to self-weight and superimposed loads. By systematically varying boundary conditions and modeling strategies, this study assess how support constraints influence thrust line equilibrium, stress redistribution, and overall stability. The results show how sensitive URM vaults are to support conditions and offer insights into contemporary methods for evaluating historical masonry structures.

Large-scale historical monuments frequently have masonry structures. Iconic structures include the Gothic Ribbed Vaults of European Cathedrals, the Pantheon and the Basilica of Maxentius, Rome, alongside India's colossal dome at the Global Vipassana Pagoda demonstrate the versatility and longevity of URM structures over centuries. These are typically constructed using materials like stone, brick, and lime mortar, which exhibit high compressive strength but negligible tensile resistance (Heyman 1966).

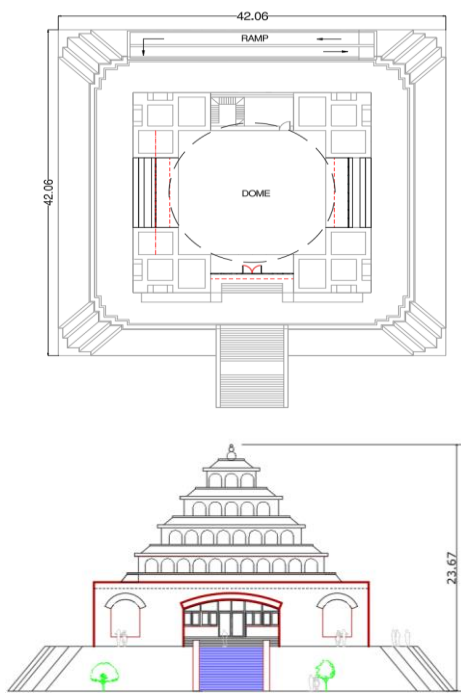


Fig. 1. Plan and Elevation of Structure

TABLE II. Mechanical Material Properties

	Value	Unit
Young's Modulus	3270	Mpa
Density	2400	N/m ³
Poisson's Ratio	0.15	

II. PROPOSED METHODOLOGY

In this study, a post-processing methodology is proposed to derive thrust lines from linear elastic finite element stress results for masonry vaults. The structural response of the vault is first obtained using ANSYS APDL, and the resulting data are then used in FETLA to construct and visualize the corresponding thrust lines.

The procedure begins with a detailed evaluation of the total superimposed structural load acting on the vault. To accurately determine the portion of the load carried exclusively by the vault, representative nodal points on the vault surface are identified and used to extract the vertical reaction and load components.



Fig. 2. Actual Image of Structure

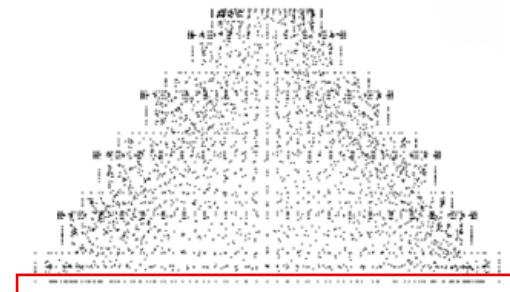


Fig. 4. Selection of nodes from 3D model

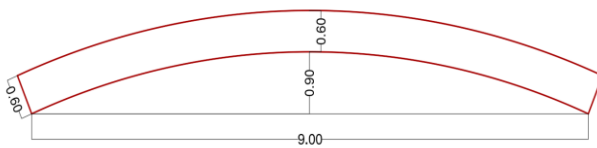


Fig. 3. Geometry of the Vault

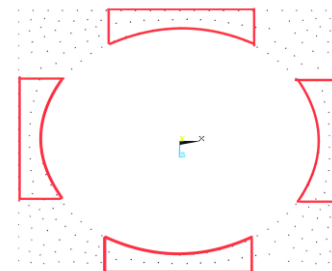


Fig. 5. Top view of selected nodes

TABLE I. Vault Dimensions

	Value	Unit
Span	0.9	M
Rise	0.9	M
Thickness	0.6	M

By restricting the load quantification to the selected vault nodes, the influence of adjacent structural elements is excluded and a more reliable estimate of the true vault loading is achieved.

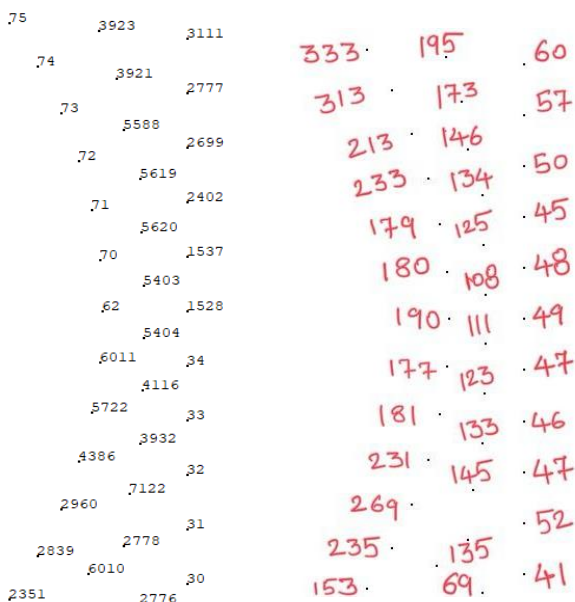


Fig. 6. Nodal numbering for vault representation

Fig. 7. Vertical (Fy) reactions

Sum of total (Fy) reaction = **5026 kN**

A. UNIFORM VERTICAL LOAD DISTRIBUTION

For the application of vertical forces, the total computed load was uniformly distributed by dividing it into 24 equal nodes, ensuring an even and accurate load application across the vault structure.

$$\begin{aligned}
 \text{Applied loads on each nodes} &= \frac{\text{Total vertical load}}{\text{Width} * \text{No. of nodes}} \\
 &= \frac{5026 * 1000}{2 * 24} \\
 &= \underline{\underline{\text{104708 N}}}
 \end{aligned}$$

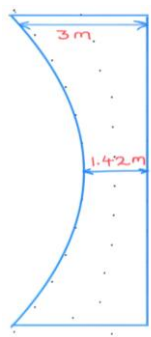
----- Applied (F_y) load on each node

Note:

As the corner width is **3m** and the central width is **1.42m**, the average width was considered for analysis and modelling.

The calculated average width is:
 $(3m + 1.42m) / 2 = 2.21m$.

Therefore, a representative width of **2m** was adopted for the analysis.



B. DEVELOPMENT OF 2D FEA MODEL FOR VAULT ANALYSIS

After calculating the total vertical force acting on the vault, a 2D analytical approach adopted to achieve higher computational precision while ensuring compatibility with FETLA, which operates exclusively in a 2D modeling framework.



Fig. 8. Considered vault section



Fig. 9. 2D model of the vault (Line Support)

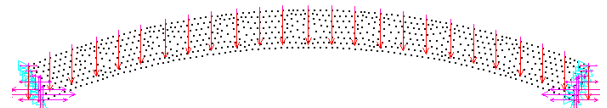


Fig. 10. Application of loads on 2d model

FEA Stress Results:

The FEA stress results indicate fixed-end beam-like behavior under both dead load and imposed load conditions, as illustrated in the figure.

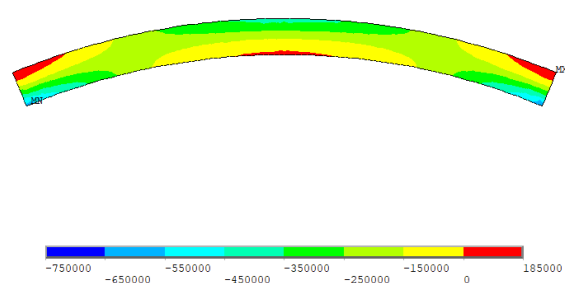


Fig. 11. Meridional Direction Stresses (Dead Load)

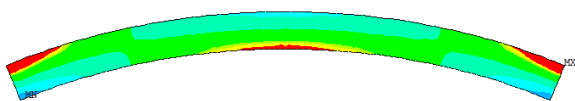


Fig. 12. Meridional Direction Stresses
 (Imposed Load)

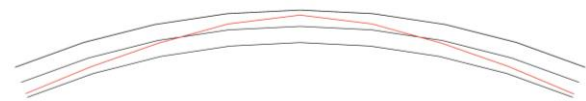


Fig. 17. Thrust Line (1st Iteration) (Dead Load)



FETLA Results:

Ten iterations were performed in the FETLA code to evaluate the behavior and convergence of the Thrust line.

As shown in the figure, the red color represents meridional stresses in compression, while the blue color denotes meridional stresses in tension.

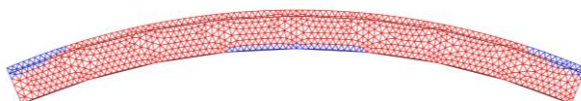


Fig. 13. Element Stresses (1st iteration)
 (Dead Load)

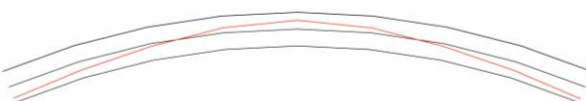


Fig. 18. Thrust Line (10th Iteration) (Dead Load)

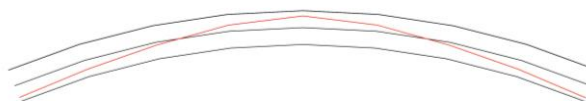


Fig. 19. Thrust Line (1st iteration)
 (Imposed Load)

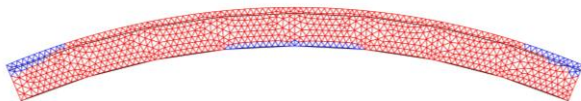


Fig. 14. Element Stresses (10th iteration)
 (Dead Load)

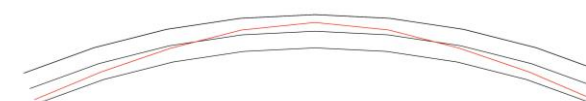


Fig. 20. Thrust Line (10th iteration)
 (Imposed Load)

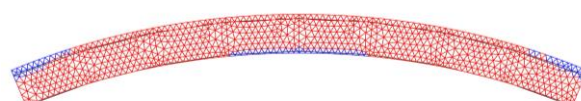


Fig. 15. Element Stresses (1st iteration)
 (Imposed Load)

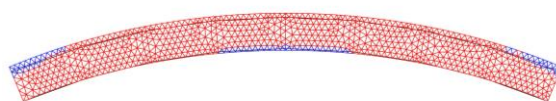


Fig. 16. Element Stresses (10th iteration)
 (Imposed Load)

C. EFFECT OF BOUNDARY CONDITION VARIATIONS

The boundary conditions will now be modified to observe the resultant changes in stresses and thrust line behavior. Previously, the supports were constrained along the full width of the vault. In the current step, the support is applied solely at the central nodes, with constraints imposed on two degrees of freedom FX and FY.

By reassessing the structural response under these constraints, the objective is to determine whether the results remain consistent or exhibit significant variations, thereby enhancing the accuracy and reliability of the assessment.



Fig No: 21- 2D model of the vault (nodal central point support) (DL Only)



Fig. 26. Element Stresses (10th iteration) (Dead Load)

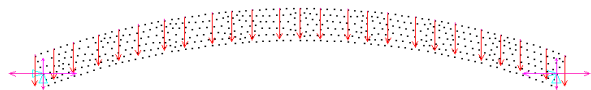


Fig No: 22- Application of loads on 2d model (Imposed Load)



Fig. 27. Element Stresses (1st iteration) (Imposed Load)

FEA Stress Results:



Fig No: 23- Meridional Direction Stresses (Dead Load)

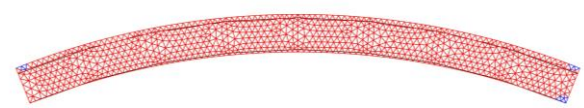


Fig. 28. Element Stresses (10th iteration) (Imposed Load)

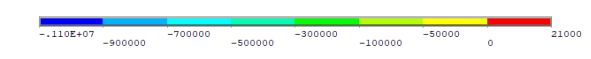


Fig No: 24- Meridional Direction Stresses (Imposed Load)



Fig. 29. Thrust Line (1st Iteration) (Dead Load)

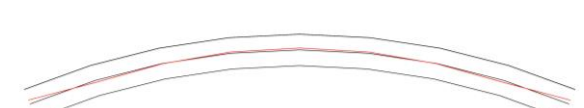


Fig. 30. Thrust Line (10th Iteration) (Dead Load)



Fig. 25. Element Stresses (1st iteration) (Dead Load)

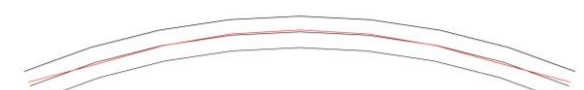


Fig. 31. Thrust Line (1st Iteration) (Imposed Load)

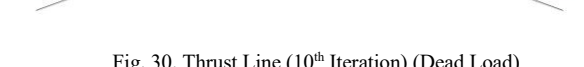


Fig. 32. Thrust Line (10th Iteration) (Imposed Load)

III. RESULT

The final result of the study show that the boundary conditions have a significant impact on the structural behavior of the vault. When supports are along the full width (line support), the thrust line extended beyond the middle third of the section and tensile stresses developed, indicating instability and a fixed beam like behavior. However, when the support was applied only at the central nodes with two degrees of freedom constrained, the thrust line remained within the middle third, tensile stresses reduced, and the vault shows improved stability. This demonstrates that modeling the vault with nodal midpoint support yields a more realistic and stable structural response, aligning with Heyman's middle third rule for masonry stability.

IV. CONCLUSION

This study demonstrates that Thrust Line behavior in URM vault is sensitive to support conditions, with significant implication for stability and load distribution. If the Thrust Line falls outside the middle third zone, tension is induced in the masonry, which it cannot resist effectively due to its brittle nature. This leads to cracking, hinge formation, and potentially progressive collapse of the structure.

When the vault supported along the full width (line support), the thrust line extended beyond the middle third of the section and tensile stresses developed, indicating instability and a fixed beam-like behavior. However, when the support was applied only at the central nodes with two degrees of freedom constrained, the thrust line remained within the middle third, tensile stresses reduced, and the vault exhibited improved stability. This demonstrates that modeling the vault with nodal mid-point support yields a more realistic and stable structural response, aligning with Heyman's middle third rule for masonry stability

Additionally, strain energy distribution remains identical for both compression and tension, which is inconsistent with material-specific mechanical behavior, highlighting a potential limitation of the current modelling approach. The results underscore the necessity of employing advanced FEM methodologies for accurate structural assessment and stability prediction.

REFERENCES

- [1] Block, P., Ciblac, T., and Ochsendorf, J. (2006). "Real time limit analysis of vaulted masonry buildings." *Computers and Structures*, 84, 1841–1852.
- [2] Buhan, P., and Felice, G. (1997). "A homogenization approach to the ultimate strength of brick masonry." *J. Mech. Phys. Solids*, 45, 1085–1104.
- [3] Cecchi, A., and Marco, R. (2002). "Homogenized strategy towards constitutive identification of masonry." *Journal of Engineering Mechanics*, 128, 688–697.
- [4] Clemente, P., Ochiuzzi, A., and Rattal, A. (1995). "Limit behavior of stone arch bridges." *Journal of Structural Engineering*, 121, 1045–1050.
- [5] Heyman, J. (1967). "On shell solutions of masonry domes." *International Journal of Solids and Structures*, 3, 227–241.
- [6] Heyman, J. (1969). "The safety of masonry arches." *International Journal Mech. Sci.*, 11, 363–385.
- [7] Milani, G., Lourenço, P., and Tralli, A. (2006). "Homogenised limit analysis of masonry walls, Part I: Failure surfaces." *Computers and Structures*, 84, 166–180.
- [8] O'Dwyer, D. (1999). "Funicular analysis of masonry vaults." *Computers and Structures*, 73, 187–197.
- [9] Pegon, P., Pinto, A., and Geradin, M. (2001). "Numerical modelling of stone-block monumental structures." *Computers and Structures*, 79, 2165–2181.
- [10] The ANSYS software website. [Online]. Available: <http://www.ansys.com/>
- [11] Varma, M., Jangid, R. S., and Ghosh, S. (2010). "Thrust line using linear elastic finite element analysis for masonry structures." *Advanced Materials Research*, 133–134, 503–508.
- [12] Heyman, J. (1995). "The Stone Skeleton: Structural engineering of masonry architecture." *Cambridge University Press*, Cambridge.
- [13] Huerta, S. (2001). "Mechanics of masonry vaults: The equilibrium approach." In *Proceedings of the Historical Constructions Conference*, Guimarães, 47–70.
- [14] Galassi, S., and Tempesta, G. (2021). "The safety of masonry arches subject to vertical and horizontal forces: A numerical method based on the thrust line closest to the geometrical axis." *International Journal of Masonry Research and Innovation*, 6(4), 298–320.